Available online at www.sciencedirect.com
ScienceDirect
Computational Materials Science 39 (2007) 767–774
COMPUTATIONAL MATERIALS SCIENCE
www.elsevier.com/locate/commatsci

A three-dimensional model for particle dissolution in binary alloys

F.J. Vermolen [a,*], E. Javierre [a], C. Vuik [a], L. Zhao [b,c], S. van der Zwaag [d]

[a] Delft University of Technology, Delft Institute of Applied Mathematics, Mekelweg 4, 2628 CD Delft, The Netherlands
[b] Delft University of Technology, Department of Materials Science and Engineering, Mekelweg 2, 2628 CD Delft, The Netherlands
[c] Netherlands Institute for Metals Research, Mekelweg 2, 2628 CD Delft, The Netherlands
[d] Delft University of Technology, Department of Aerospace Engineering, Kluyverweg 1, 2629 HS Delft, The Netherlands

Received 13 September 2006; accepted 20 September 2006

Abstract

A three-dimensional model for particle dissolution in binary alloys is proposed and its numerical solution procedure is described. The model describes dissolution of a stoichiometric particle as a Stefan problem. The numerical method is based on a level set method, which has a wide applicability in modeling moving boundary problems. The present model relies on local thermodynamic equilibrium on the interface between the dissolving particle and the diffusive phase. The level set method is shown to handle complex topological changes in particle break-up very well. The potential of the technique is demonstrated in describing the globularization of planar, perturbed and cracked cementite plates in a pearlitic microstructure.

Keywords: Binary alloy; Particle dissolution; Moving interfaces; Diffusion; Level set method; Spheroidization

1. Introduction

Particle growth or dissolution is a common metallurgical process. Due to the scientific and the industrial relevance of being able to predict the kinetics of particle dissolution, many models of various complexity have been presented and experimentally validated. The early models on particle dissolution and growth based on long-distance diffusion consisted of analytic solutions in an unbounded medium under the assumption of local equilibrium at the interface, see Ham [1,2], Zener [3], Whelan [4] and Aaron and Kotler [5] to mention just a few. The model of Nolfi et al. [6] incorporates the interfacial reaction between the dissolving particle and its surrounding phase. Later, modeling of particle dissolution has been extended to the introduction of multi-component particles by, among others, Andersson and Ågren [7], Ågren [8], Ågren and Vassilev [9], Thornton et al. [10], Reiso et al. [11], Hubert [12], Vitek et al. [13], Vusanović and Krane [14], Atkinson et al. [15] and Vermolen et al. [16,17]. Bourne et al. [18] treat the growth of ellipsoidal phases in ternary systems. In these papers particle dissolution was viewed as a Stefan problem with a sharp interface separating the constitutive phases.

An alternative approach to particle dissolution is the phase-field approach, which is derived from a minimization of a free energy functional employing a diffuse interface between the phases in contact. This approach has been used by Kobayashi [19], among others, to simulate dendritic growth. An extension to multi-component phase-field computation is done by Grafe et al. [20], where solidification and solid state transformations are modeled. For a one-dimensional case they obtain a perfect agreement for one spatial dimension between the phase-field approach and the software package DICTRA, which is based on a sharp interface between the consecutive phases. Recently, Kovačević and Šarler [21] also obtained a perfect agreement for dissolution of Al_2Cu precipitates in an aluminum alloy between a phase-field approach and sharp interface

* Corresponding author. Tel.: +31 15 2787298; fax: +31 15 2787209.
E-mail address: F.J.Vermolen@tudelft.nl (F.J. Vermolen).

0927-0256/$ - see front matter © 2006 Elsevier B.V. All rights reserved.
doi:10.1016/j.commatsci.2006.09.009

(Stefan) approach where a moving grid method and a meshfree method was used. However, some drawbacks of the phase-field approach are the following: no quick analytic estimate of the solution is available, the diffuse interface is physically unrealistic and physically justifiable parameter values in the energy functional are hard to get. Generally, these values are derived from fitting simulations to experiments. Derivation of these parameters from the information available in thermodynamic databases is generally not yet possible. An other drawback for the phase-field model is that a very fine grid resolution in the diffuse interface is necessary in order to capture the interface such that an agreement with the 'sharp interface method' is obtained. This poses a severe requirement on the time-step and hence large computation times result. This was noted in the numerical literature by Burman et al. [22] and Javierre et al. [23]. We also note that the use of a lower resolution of the mesh in the diffuse interface gives qualitatively reasonable solutions, however, from a quantitative view the simulations do not agree with the 'sharp interface model'. The numerical methods to the phase-field problem used by Burman et al. [22], MacKenzie and Robertson [24] and Javierre et al. [23] were based on an adaptive grid distribution so that the resolution in the interfacial region is sufficiently fine. The use of such an adaptive grid poses numerical problems which we avoid by modeling particle dissolution as a Stefan problem with a sharp interface separating the adjacent phases and using the level set method to compute the solution. The review paper by Thornton et al. [10] presents a nice overview of the various diffuse and sharp interface models for diffusional transformations.

Several numerical methods exist for solving Stefan problems with a sharp interface related to particle dissolution and phase transformations. A survey on classical numerical methods for Stefan problems is given by Crank [25]. The most commonly used methods to solve Stefan problems are the moving grid method and fixed grid methods. The one-dimensional moving grid method was introduced by Murray and Landis [26] and improved for solid state transformations by Ågren and Vassilev [9] and Crusius et al. [27]. In these last papers more effort was put into global mass conservation of the numerical solution. Segal et al. [28] extended the moving grid method, to solve the particle dissolution problem, to a two-dimensional Finite Element framework. So far no three-dimensional models have been presented involving moving grids in the metallurgical literature.

In the present paper we employ a fixed grid in combination with the advanced level set method to capture particle dissolution in three spatial dimensions. This method was introduced by Osher and Sethian [29] and later described in a general way by Sethian [30] and by Osher and Fedkiw [31]. It was firstly applied to a Stefan problem for solidification with two spatial dimensions by Chen et al. [32]. The level set method turns out to be very suitable for extension to problems with three spatial dimensions. The method also allows problems with topological changes of the phases present to be dealt with in a natural way. A comparative study of the level set method, moving mesh technique and phase-field method is due to Javierre et al. [23] for one spatial co-ordinate. A comprehensive comparison between the level set method and the moving grid method for two and three-dimensional problems is presented elsewhere [33]. Although the level set method has been applied to solidification problems several times, it has not yet been applied to solid state phase transformations such as the dissolution of second phase particles. In contrast to the present solid state models for particle dissolution which only yield shape and topology preserving solutions, it is our aim in this paper to apply the level set method to three-dimensional particle dissolution where both the shape and topology of the dissolving phases are part of the solution to be obtained. These topological changes allow breaking up of particles in a natural way, which is a novelty for the sharp interface (Stefan) models. To illustrate the capability of our method of dealing with topological changes, we apply our approach to the spheroidization of cementite plates in pearlite structures in steels. The spheroidization was simulated using a modified fault migration theory due to Tian and Kraft [34]. The microscopic images of Hernandéz-Silva et al. [35] provide the necessary experimental evidence for the occurring spheroidization process.

In this study we first introduce the three-dimensional model for particle dissolution in a binary alloy. Subsequently the level set method is introduced and applied to the dissolution of pre-cracked cementite plates in a binary Fe–C alloy. Furthermore, a discussion on the model is presented and finally, some conclusions are drawn.

2. The model

The microstructure for this simulation is simplified into a representative cell containing a stoichiometric β particle with a given shape surrounded by an α-diffusive phase in which the alloying element diffuses. Both a uniform and spatially varying initial concentration at $t = 0$ can be dealt with in the model. The boundary between the particle and diffusive phase is referred to as the interface. Particle dissolution is assumed to proceed via the following steps: decomposition of the particle, passage of the atoms composing the particle through the interface and finally long-distance diffusion of the atoms into the surrounding phase. In the present paper we assume long-distance diffusion to control the interface motion, *i.e.* local thermodynamic equilibrium is assumed at the interface and hence the interface concentration is the concentration as predicted by the thermodynamic phase diagram at the annealing temperature. Further, we assume that the particle concentration is constant all over the particle and at all stages of the dissolution process.

We denote the interface, consisting of a point, curve or a surface for respectively a one-, two- or three-dimensional domain of computation by $S = S(t)$. The outer (fixed)

boundaries of the domain of computation are denoted by Γ. Further, the domain of computation is split into the matrix or diffusive part (the α-diffusive phase), denoted by Ω and the β-particle Ω_p. The distribution of the alloying element is determined by diffusion in the diffusive phase Ω, which gives

$$\frac{\partial c}{\partial t} = D\Delta c = D\left\{\frac{\partial^2 c}{\partial x^2} + \frac{\partial^2 c}{\partial y^2} + \frac{\partial^2 c}{\partial z^2}\right\} \quad \text{for } \mathbf{x} \in \Omega(t) \text{ and } t > 0. \tag{1}$$

Here D represents the diffusion coefficient and $\mathbf{x}$ denotes the spatial position within the domain of computation. In the present study we treat D as a constant. Within the particle the concentration is equal to a given constant, hence

$$c = c^{\text{part}} \quad \text{for } \mathbf{x} \in \Omega_p(t) \quad \text{and} \quad t \geqslant 0. \tag{2}$$

On the interface, $S(t)$, we have local equilibrium, *i.e.* the concentration is as predicted by the thermodynamic phase diagram, *i.e.*

$$c = c^{\text{sol}} \quad \text{for } \mathbf{x} \in S(t) \quad \text{and} \quad t > 0. \tag{3}$$

Further, at the outer boundary, Γ, we have no flux of atoms, that is

$$D\frac{\partial c}{\partial n} = 0 \quad \text{for } \mathbf{x} \in \Gamma(t) \quad \text{and} \quad t > 0. \tag{4}$$

In the above equation $\frac{\partial c}{\partial n}$ denotes the outward normal derivative of c on the outer boundary Γ. From a local mass balance, the equation of motion of the interface can be derived, this equation is commonly referred to as the Stefan condition, and is given by

$$(c^{\text{part}} - c^{\text{sol}})v_n = D\frac{\partial c}{\partial n} \quad \text{for } \mathbf{x} \in S(t) \quad \text{and} \quad t > 0. \tag{5}$$

Here v_n denotes the normal component of the interface velocity outward from Ω. The problem is completed with the initial concentration c^0 and the initial position of the interface $S(0)$. The problem, consisting of Eqs. (1)–(5) is referred to as a Stefan problem for particle dissolution or particle growth. For the case of growth of particles, the Gibbs–Thomson effect is important in the early stages of growth after nucleation. The early-stage phenomena of nucleation differ totally from the present Stefan problem. Therefore, we do not consider particle growth in the present study. In a future study the Gibbs–Thomson effect will be implemented into the three-dimensional model and then more numerical results on particle growth will be shown.

The Stefan problem presented here is solved by the use of the level set method, which is described in the next section.

3. The level set method

The level set method has been applied successfully to a wide variety of problems with moving interfaces separating adjacent phases. An example of the application of the level set method in multi-phase flows is treated by Van der Pijl et al. [36]. In the treatment of the level set method, we follow many of the procedures described by Osher and Fedkiw [31], Chen et al. [32] and Javierre et al. [33]. For more details on numerical issues, we refer to the latter paper. The level set method that we present here is based on a fixed grid, that is the grid does not change due to the movement of the interface. As before, Fick's second law (1) is solved by the use of a Finite Element method in three dimensions. The interface, either a point, line or surface in one-, two- or three-dimensional simulations respectively, is captured by the use of the zero level set of the so-called level set function $\phi = \phi(\mathbf{x}, t)$. This function is used as an artificial function for mathematical reasons. Let Q be the total domain of computation including the diffusive phase, particle as well as the interface, *i.e.* $Q = \Omega \cup \Omega_p \cup S$, then, the interface is described by

$$S = S(t) := \{\mathbf{x} \in Q \text{ for which } \phi(\mathbf{x}, t) = 0\}. \tag{6}$$

In other words, at a time t we have $\phi(\mathbf{x}, t) = 0 \iff \mathbf{x} \in S(t)$ (*i.e.* $\phi = 0$ on the interface $S(t)$). This implies, on each point of the moving interface $\mathbf{x} \in S(t)$, that the following total (material) derivative of the level set function is zero, *i.e.*

$$0 = \frac{\mathrm{d}\phi}{\mathrm{d}t} = \frac{\partial \phi}{\partial t} + \frac{\mathrm{d}\mathbf{x}}{\mathrm{d}t} \cdot \nabla \phi \quad \text{for } \mathbf{x} \in S(t), \tag{7}$$

since the level set function $\phi = 0$ on the interface $S(t)$ at all stages of the phase-transformation. In the above equation $\frac{\mathrm{d}\mathbf{x}}{\mathrm{d}t}$ represents the velocity of the interface at a point $\mathbf{x}$ on the interface. To monitor the zero level set of the function ϕ, Eq. (7) is solved over the whole domain Q with a continuously extended velocity $\mathbf{v}$ from the interface velocity in Eq. (7). We will come back to the continuous extension of the velocity $\mathbf{v}$ later. This leads to the following convection equation for ϕ on the entire domain of computation Q:

$$\frac{\partial \phi}{\partial t} + \mathbf{v} \cdot \nabla \phi = 0. \tag{8}$$

At time $t = 0$ the level set function ϕ is initialized as a 'signed distance function' by

$$\phi(\mathbf{x}, 0) = \begin{cases} +\text{dist}(\mathbf{x}, S(0)) & \text{for } \mathbf{x} \in \Omega(0), \\ 0 & \text{for } \mathbf{x} \in S(0), \\ -\text{dist}(\mathbf{x}, S(0)) & \text{for } \mathbf{x} \in \Omega_p(0). \end{cases} \tag{9}$$

By which we mean that at each point of the diffusive phase Ω the level set function initially is given the value of the distance between the point and the closest initial interface position. For the points in the particle phase Ω_p the same holds but then with opposite sign. On the interface the level set function is given the initial value of zero. For the case that $\mathbf{v} = \mathbf{v}(\mathbf{x}, t)$ is known at all times and on each location of the computational domain Q, Eq. (8) can be solved with the initial condition 9. In general, as time proceeds, the level set function ϕ is no longer a distance function after solution of Eq. (8). The level set function ϕ is used to determine the interface position, therefore ϕ has to be continu-

ous. Further, for convenience for the discretization of the gridpoints that neighbor the interface, the level set function is adapted such that it is or approximates a signed distance function at all stages of the phase-transformation. This adaptation is referred to as re-initialization, which was introduced by Sussman et al. [37] and applied to a Stefan problem by Chen et al. [32]. The re-initialization procedure relies on the solution of

$$\frac{\partial \psi}{\partial \tau} = \mathrm{Sign}(\phi(\mathbf{x},t))(1 - \|\nabla \psi(\mathbf{x},\tau)\|), \tag{10}$$

in an artificial time τ, with initial condition $\psi(\mathbf{x},0) = \phi(\mathbf{x},t)$. Eq. (10) guarantees that whenever $\phi = 0$, then, $\psi = 0$, *i.e.* the zero level set of ϕ and ψ are the same. The steady-state solution of the above equation is given by $\|\nabla\psi\| = 1$, which is a characteristic of a distance function. After solution of Eq. (10) to obtain ψ as a signed distance function, we set $\phi = \psi$. If necessary, this can be done at several time-steps, see Javierre et al. [33]. There is an abundant variety of solution methods of Eq. (10), see for instance Osher and Fedkiw [31]. We remark that there the re-initialization procedure is done such that within a narrow bandwidth of several meshsizes around the interface, the level set function indeed approximates a signed distance function. It is only there where this is important. At locations far away from the interface, only the sign of the level set function matters.

Now the extended velocity enters the picture. The level set function ϕ can only be transported, using Eq. (8), if the velocity of the interface is extended continuously to obtain $\mathbf{v}$ over the entire domain of computation Q. At the interface, the velocity is determined by the Stefan condition for the interface, see Eq. (5). Following Chen et al. [32], this velocity is split into the x, y and z components to serve as boundary conditions for the following three partial differential equations for the components of $\mathbf{v}$, respectively denoted by v_x, v_y and v_z

$$\begin{cases} \dfrac{\partial v_x}{\partial \tau} + \mathrm{Sign}\left(\phi \dfrac{\partial \phi}{\partial x}\right) \dfrac{\partial v_x}{\partial x} = 0, \\ \dfrac{\partial v_y}{\partial \tau} + \mathrm{Sign}\left(\phi \dfrac{\partial \phi}{\partial y}\right) \dfrac{\partial v_y}{\partial y} = 0, \\ \dfrac{\partial v_z}{\partial \tau} + \mathrm{Sign}\left(\phi \dfrac{\partial \phi}{\partial z}\right) \dfrac{\partial v_z}{\partial z} = 0. \end{cases} \tag{11}$$

Here τ represents again a pseudo-time. Note that the components of $\mathbf{v}$ are given at the interface, which is used as a boundary condition for the above equations. The above strategy for the extension of the interface velocity onto the whole domain of computation is referred to as the Cartesian extension, as proposed by Chen et al. [32] for a Stefan problem. The sign-function in the above equation takes care of numerical convection in the proper upwind direction.

In the present approach the diffusion Eq. (1) is solved using a three-dimensional Galerkin Finite Element method. The elements neighboring the interface are cut into additional elements, this method is referred to as the cut-cell approach. We remark that the cut-cell method never alters the level set function. Further, when the interface crosses a node, the time-stepping is adapted locally. These issues is described in more detail in Javierre et al. [33] since the aim of the present paper is to show the possible applications of our model. The equations for the level set function (8), and the extended velocity (11) are solved using a three-dimensional first-order upwind Finite Difference technique. The re-initialization problem (10) is solved using a higher-order three-dimensional Finite Difference technique.

4. Metallurgical application

The metallurgical application in this section is inspired by an AISI 52100 steel, which is widely used to make hardened components such as bearings, gears, transmission shafts, *etc.* due to its excellent properties. The steel contains mainly 1.0 wt.% of carbon and 1.36 wt.% of chromium. The diffusion of chromium is neglected in this study and hence we treat the alloy as a binary alloy by considering the diffusion of carbon only. In Zhao et al. [38] the diffusion of carbon and chromium is treated for a dissolving spherical cementite particle. This physically justifiable binary assumption is made as the present model is not yet capable of dealing with a multiple alloying elements. In this study, we simulate the spheroidization process of dissolving lamellar pearlite structure, which is the major part of the soft annealing process in order to make the steel machinable. It is worth noting that all thermodynamic data are calculated using the MTData software. Further, we remark that the calculations serve to illustrate our method and not to quantitatively compute the cementite dissolution in the realistic AISI 52100 steel since the diffusion of chromium is not incorporated in the present model due to the binary assumption. Hence, the present calculations are for a hypothetic alloy.

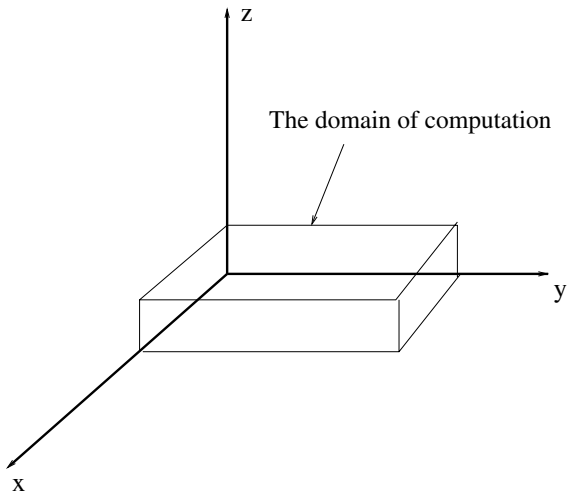

Fig. 1. The used co-ordinate system.

Consider a planar cementite phase surrounded by a planar ferrite matrix. The used co-ordinate framework is given in Fig. 1. The lamellae structure of pearlite is simplified into one cementite plate for reasons of symmetry. We consider a perturbation for the planar particle in the form of a knucklebone shape [39]. We assume that the voids in the knuckelbone shape are filled by the ferrite phase entirely. The configuration is shown in Fig. 2. In this section the temperature has been chosen at 800 °C > 789 °C, which is the finish temperature of ferrite dissolution [38], and the plate dimensions of $0.1 \times 1 \times 5\ \mu m^3$ have been used. The plate dissolves in a computational cell with dimensions $0.5 \times 2.4 \times 5\ \mu m^3$. Hence the initial volume fraction of the dissolving plate is 8.33%. The model essentially deals with the dissolution of a cementite plate in an austenite matrix. The concentration of carbon within the cementite particle is given by $c^{\theta} = 6.743$ wt.%. Further, the initial carbon composition in the ferrite matrix, which is 'inherited' by the austenite upon its first formation, is set at 0 wt.%. We note that the overall carbon concentration in the alloy is less than 1.0 wt.%, which holds for the AISI 52100 steel. We chose this in order to be able to visualize the complete dissolution of the plates including breaking up into subplatelets as the dissolution process proceeds. The concentration at the interface between the cementite and ferrite phases is set equal to the value that follows from local equilibrium at $T = 800$ °C, given by $c^{\gamma/\theta} = 0.71719$ wt.%. For the diffusion coefficient the value $D = 2.98\ \mu m^2/s$ [40, p. 99] is used, corresponding to the temperature of 800 °C.

It can be seen in Figs. 3 and 4 that the planar particle gradually splits up into adjacent particles and as time proceeds the particles become more and more spheroidized and will dissolve either partly or entirely. This is an example of a feature that can be dealt with rather easily when using the level set method. The moving mesh method would complicate matters very much when modeling this phenomenon. The importance of breaking up of dissolving phases is illustrated in the measurements by [35].

To get more insight from the simulations that have been done for the dissolving cementite plate, cross-sectional profiles parallel to the z-axis at consecutive times have been plotted in Fig. 5. The displacement of the interface with respect to its original position varies both locally (for each sub unit in the plate) and macroscopically (edge units

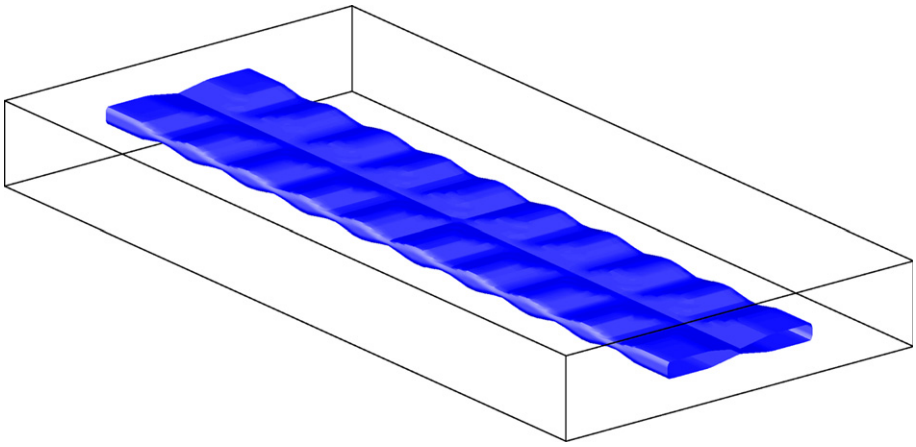

Fig. 2. The initial cementite plate with a knucklebone shape.

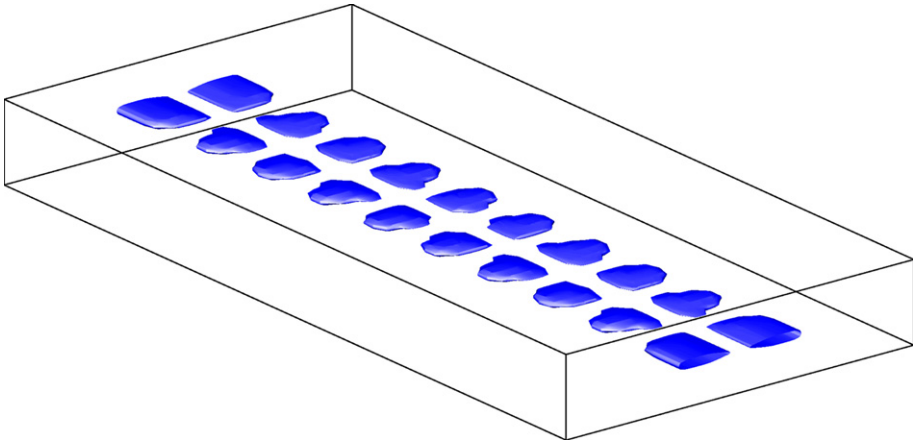

Fig. 3. The cementite plate, initially as in Fig. 2, after 52 time-steps at $t = 0.009$.

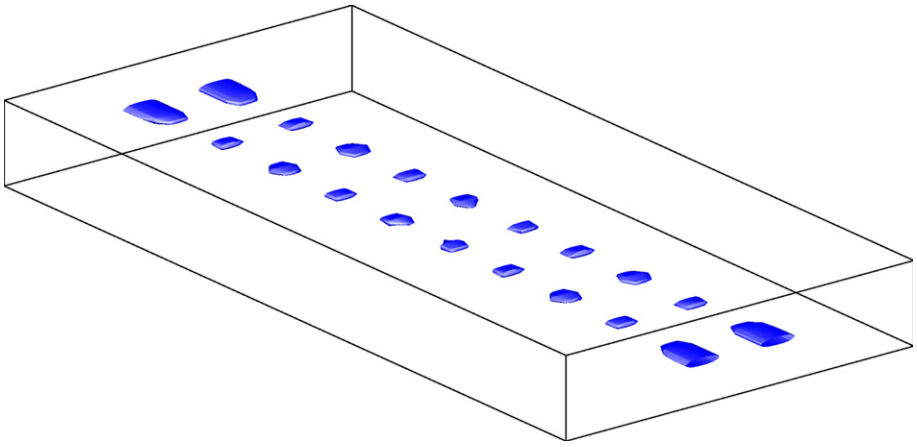

Fig. 4. The cementite plate, initially as in Fig. 2, after 78 time-steps at $t = 0.016$.

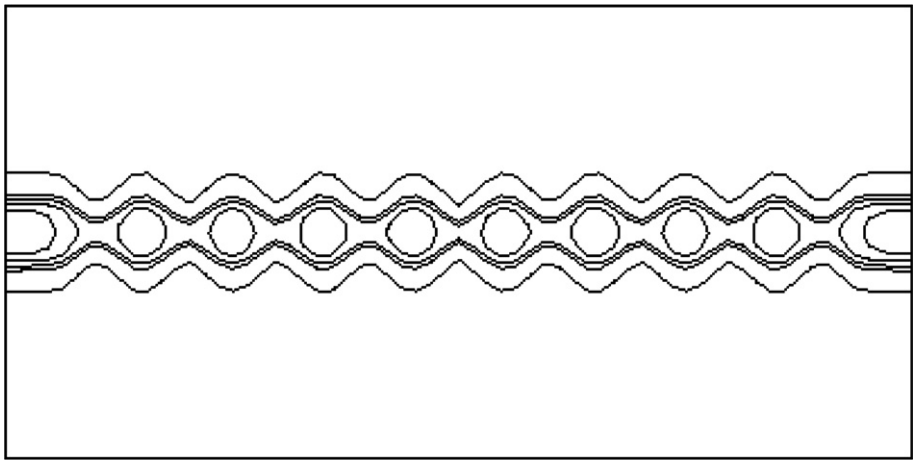

Fig. 5. An intersection parallel to the yz-plane at $x = 0.95$ of the interfacial position at consecutive times ($t = 0$, 0.02, 0.04 and 0.06). The most upper and most lower curves denote the intersection at $t = 0$ and the calculation was done for a plate with linear cracks and its thickness was adjusted to have an initial volume fraction of 8.33%.

behave differently to center units). Furthermore, the initially non-smooth edges get rounded off during the dissolution process.

Next we present the normalized volume ($V(t)/V_0$, where V_0 is the initial particle volume of the unperturbed plate) of the cementite as a function of the normalized dissolution time (t/t_{diss}, where t_{diss} denotes the time of complete dissolution of the unperturbed plate) for several cases. The results have been plotted in Fig. 6. The cases that we treat in the order of decreasing dissolution time all start with the same initial particle volume. The first case corresponds to the unperturbed plate. The second case is based on a collection of 20 platelets whose thickness have been enlarged to have the total initial volume be equal to the volume of the unperturbed plate in case 1, that is 8.33%. The third case represents a planar particle with linear cracks and the plate has been made thicker (that is its size has been enlarged in the z-direction) to have the same initial particle volume as in case 1. The fourth and last case corresponds to a plate perturbed with linear cracks and here the plate has been made wider (that is its size has been enlarged in the x-direction) to have the same initial plate volume as in the unperturbed case, *i.e.* the initial volume fraction is 8.33%. From the simulations it is clear that the cracks give an acceleration of the dissolution of the cementite plate, which is also commonly known in the metal processing community. For the last case, where the thickness has not been enlarged, the dissolution speed is almost three times as large as the dissolution speed of the unperturbed plate. Note that the thickness of the particles in case 2 is larger than the thickness of the unperturbed plate, which explains why the reduction of the dissolution time is relatively small.

Subsequently, we present the dissolution time of several individual particles for a set of 20 neighboring particles. The used configuration and numbering of the particles is sketched in Fig. 7. The dissolution kinetics are plotted in Fig. 8 (*viz.* the second case in Fig. 6). Here we follow the dissolution kinetics for an edge particle, and its first neighbor and one of the central particles. Since the part of the

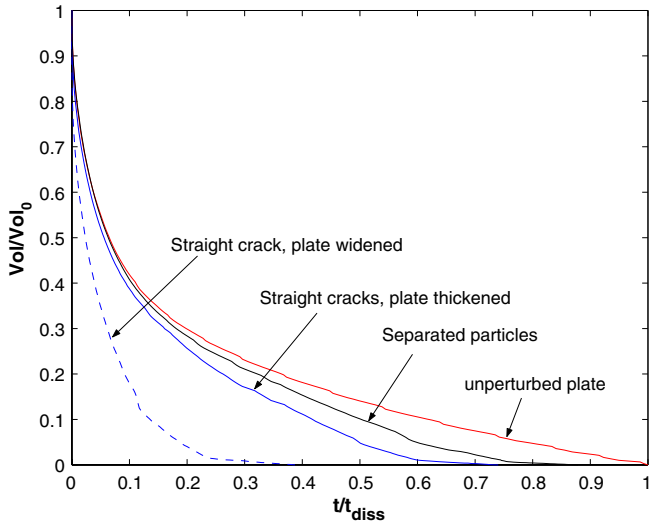

Fig. 6. The volume of the cementite plate as a function of time for several cases explained in the text.

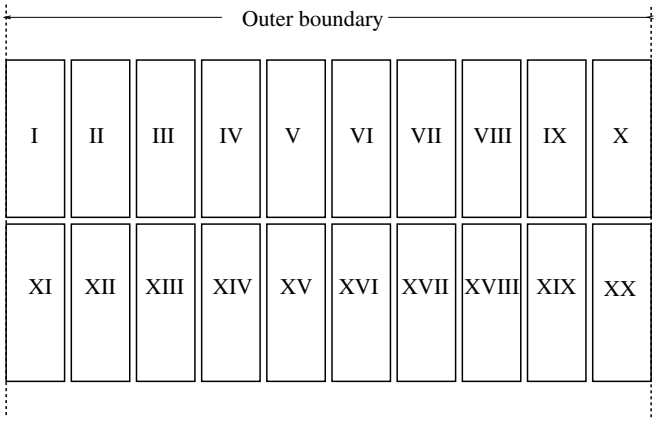

Fig. 7. The configuration and numbering of the dissolving isolated particles as an intersection at $z = 2.5$.

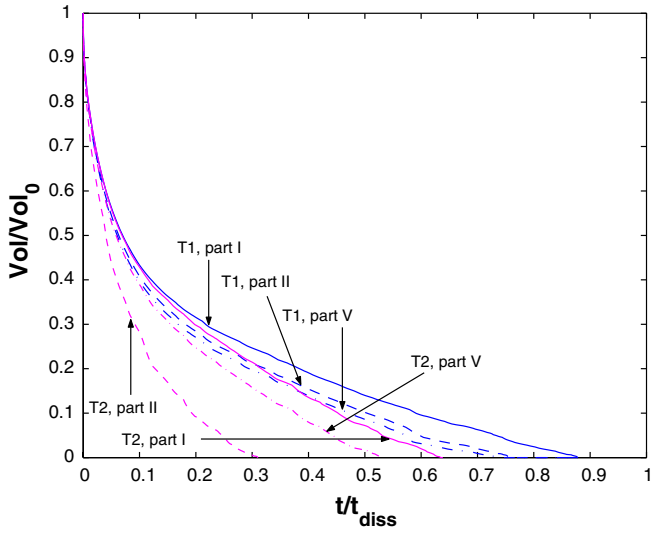

Fig. 8. The volume of several individual cementite particles as a function of time for the case of 20 particles (see T1) and for 16 particles in which particles III, VIII, XIII and XVIII have been removed (see T2).

boundary of the edge particles is on a no-flux boundary (see Fig. 7) and hence the atoms that flow out of the particle can hardly travel in the y-direction, its dissolution speed is reduced compared to the dissolution speed of the inner particles. This is seen in the curves indicated by T1. The simulations of the curves labeled with T2 are done for the case that the 3rd, 8th, 13th and 18th particles have been removed. It can be seen that the second particle dissolves fastest here due to the free space between the second and fourth particles.

5. Discussion

The presently used numerical procedure has been checked on convergence and consistency using the exact self-similar solution for an unbounded diffusive phase, the global mass balance and subsequent grid and time-step refinement. Furthermore, the geometric aspects of the initial particle geometry can be put into the model. The model is also capable of dealing with splitting of phases into dissolving particles, occurring in several metallurgical situations. This is a key innovation with respect to earlier models.

Of course, the model is not perfect and many improvements remain to be done. It is only suitable for binary alloys and the Gibbs–Thomson effect has not yet been implemented either. For the case of dissolution of our stoichiometric particle the effects due to the surface tension are relatively small. However, we realize that the Gibbs–Thomson effect may have a significant influence on the rate of splitting of the planar phase into spheroidized particles. Mathematically, this has been investigated by the use of spherical harmonics as the solution of the steady-state diffusion equation around a spherical particle by Mullins and Sekerka [41].

Moreover, the present model is based on the assumption of local equilibrium at the interface, *i.e.* the concentration at the interface is as predicted by the thermodynamic phase diagram. Some papers where the assumption of local equilibrium is relaxed are due to Sietsma and van der Zwaag [42], Svoboda et al. [43], Vuik et al. [44], Vermolen and Van der Zwaag [45] and Nolfi et al. [6]. However, for some cases of precipitates in metallic alloys, local equilibrium models describe particle dissolution accurately. This has been verified for Si particles in Aluminum alloys by Tundal and Ryum [46] and Vermolen et al. [47]. We expect local equilibrium to be a good approximation for some other alloys too, of course an experimental validation is of crucial importance here.

An approximation of the dissolution of particles in a multi-component alloy can be constructed by the use of the effective diffusivity and solubility as treated in [16]. However, the evolution of the interface concentrations as time proceeds during the dissolution process is not taken into account, so this would only serve as a zeroth order approximation. So an extension of the present method to multi-component alloys, in which the fluxes of the alloying

elements in the vicinity of the interface are taken into account, is a topic we are working on. The real multi-component model would be capable of dealing with the influence of other (slow) alloying elements, as chromium, to predict more realistic dissolution times. We, however, think that for the case of particles dissolving in binary alloys if interfacial reactions are very fast compared to long-distance diffusion, our model is a novel approach to deal with three-dimensional issues of particle dissolution. Further, our present approach allows breaking up of particles and other geometric changes to take place.

6. Conclusions

A three-dimensional sharp interface model based on the level set method is shown to handle the complex local and macroscopic topological changes during solid state particle dissolution in a binary alloy. The level set method based model offers a more realistic description of particle dissolution than the current dissolution models enforcing shape conservation. Using physical parameters for cementite plates during austenization of a binary Fe–C alloy, the model illustrated the significant acceleration of the dissolution due to multiple fractures in the cementite plates, in accordance with experimental and industrial experience.

References

[1] F.S. Ham, Journal of Physics and Chemistry in Solids 6 (1958) 335–351.
[2] F.S. Ham, Journal of Applied Physics 30 (6) (1958) 915–926.
[3] C. Zener, Journal of Applied Physics 20 (1949) 950–953.
[4] M.J. Whelan, Metals Science Journal 3 (1969) 95–97.
[5] H.B. Aaron, G.R. Kotler, Metallurgical Transactions 2 (1971) 1651–1656.
[6] F.V. Nolfi Jr., P.G. Shewmon, J.S. Foster, Transactions of the Metallurgical Society of AIME 245 (1969) 1427–1433.
[7] J.-O. Andersson, J. Ågren, Journal of Applied Physics 72 (4) (1981) 1350–1355.
[8] J. Ågren, Journal of Physics and Chemistry of Solids 43 (4) (1982) 285–391.
[9] J. Ågren, G.P. Vassilev, Materials Science and Engineering 64 (1984) 95–103.
[10] K. Thornton, J. Ågren, P.W. Voorhees, Acta Materialia 51 (2003) 5675–5710.
[11] O. Reiso, N. Ryum, J. Strid, Metallurgical Transactions A 24A (1993) 2629–2641.
[12] R. Hubert, ATB Metallurgie 34–35 (1995) 4–14.
[13] J.M. Vitek, S.A. Vitek, S.A. David, Metallurgical Transactions A 26A (1995) 2007–2025.
[14] I. Vusanović, M.J. Krane, International Communications in Heat and Mass Transfer 29 (3) (2002) 1037–1046.
[15] C. Atkinson, T. Akbay, R.C. Reed, Acta Metallurgica et Materialia 43 (5) (1995) 2013–2031.
[16] F.J. Vermolen, C. Vuik, S. van der Zwaag, Materials Science and Engineering A A347 (2003) 265–279.
[17] F.J. Vermolen, C. Vuik, Journal of Computational and Applied Mathematics 176 (1) (2005) 179–201.
[18] J.P. Bourne, C. Atkinson, R.C. Reed, Metallurgical and Materials Transactions A 25A (1994) 2683–2694.
[19] R. Kobayashi, Physics D 63 (1993) 410–423.
[20] U. Grafe, B. Böttger, J. Tiaden, S.G. Fries, Scripta Materialia 42 (2000) 1179–1186.
[21] I. Kovačević, B. Šarler, Conference of Advances of Solidification Processes in Stockholm (2005).
[22] E. Burman, M. Picasso, J. Rappaz, Analysis and computation of dendritic growth in binary alloys using a phase-field model, Numerical Mathematics and Advanced Applications, Springer, Berlin, 2004.
[23] E. Javierre, C. Vuik, F.J. Vermolen, S. van der Zwaag, Journal of Computational and Applied Mathematics 192 (2) (2006) 445–459.
[24] J.A. Mackenzie, M.L. Robertson, Journal of Computational Physics 181 (2) (2002) 526–544.
[25] J. Crank, Free and Moving Boundary Problems, Clarendon Press, Oxford, 1984.
[26] W.D. Murray, F. Landis, Transactions ASME (C) Journal of Heat Transfer 245 (1959) 106–112.
[27] S. Crusius, G. Inden, U. Knoop, L. Höglund, J. Ågren, Zeitschrift für Metallkunde 83 (1992) 669–673.
[28] A. Segal, C. Vuik, F.J. Vermolen, Journal of Computational Physics 141 (1998) 1–21.
[29] S. Osher, J.A. Sethian, Journal of Computational Physics 141 (1988) 12–49.
[30] J.A. Sethian, Level-Set Methods and Fast Marching Methods, Cambridge University Press, New York, 1999.
[31] S. Osher, R. Fedkiw, Level-Set Methods and Dynamic Implicit Surfaces, Springer-Verlag, New York, 2003.
[32] S. Chen, B. Merriman, S. Osher, P. Smereka, Journal of Computational Physics 135 (1997) 8–29.
[33] E. Javierre, C. Vuik, F.J. Vermolen, A. Segal, A Level Set Method for Particle Dissolution in a Binary Alloy, Report at the Delft Institute of Applied Mathematics, 2005, 03–05.
[34] Y.L. Tian, R.W. Kraft, Metallurgical Transactions A 18 (1987) 1359–1369.
[35] D. Hernández-Silva, R.D. Morales, J.G. Cabañas-Moreno, ISIJ International 32 (1992) 1297–1305.
[36] S.P. van der Pijl, A. Segal, C. Vuik, P. Wesseling, International Journal of Numerical Methods in Fluids 47 (4) (2005) 339–361.
[37] M. Sussman, P. Smereka, S. Osher, Journal of Computational Physics 114 (1994) 146–159.
[38] L. Zhao, F.J. Vermolen, A. Wauthier, J. Sietsma, Metallurgical and Materials Transactions A 37A (2006) 1841–1850.
[39] K.E. Thelning, Steel and its Heat Treatment, Butterworth, London, 1975.
[40] W.D. Callister, Materials Science and Engineering, An Introduction, 4th ed., John Wiley and Sons, New York, 1997.
[41] W.W. Mullins, R.F. Sekerka, Journal of Applied Physics 34 (2) (1963) 323.
[42] J. Sietsma, S. van der Zwaag, Acta Materialia 52 (2003) 4143–4152.
[43] J. Svoboda, F.D. Fischer, P. Fratzl, E. Gamsjäger, N.K. Simha, Acta Materialia 49 (2001) 1249–1259.
[44] C. Vuik, A. Segal, F.J. Vermolen, Computation and Visualisation of Science 3 (2000) 109–114.
[45] F.J. Vermolen, S. Van der Zwaag, Materials Science and Engineering A 220 (1996) 140–146.
[46] U.H. Tundal, N. Ryum, Metallurgical Transactions A 23 (1992) 433–449.
[47] F.J. Vermolen, H.M. Slabbekoorn, S. van der Zwaag, Materials Science and Engineering A A231 (1997) 80–89.